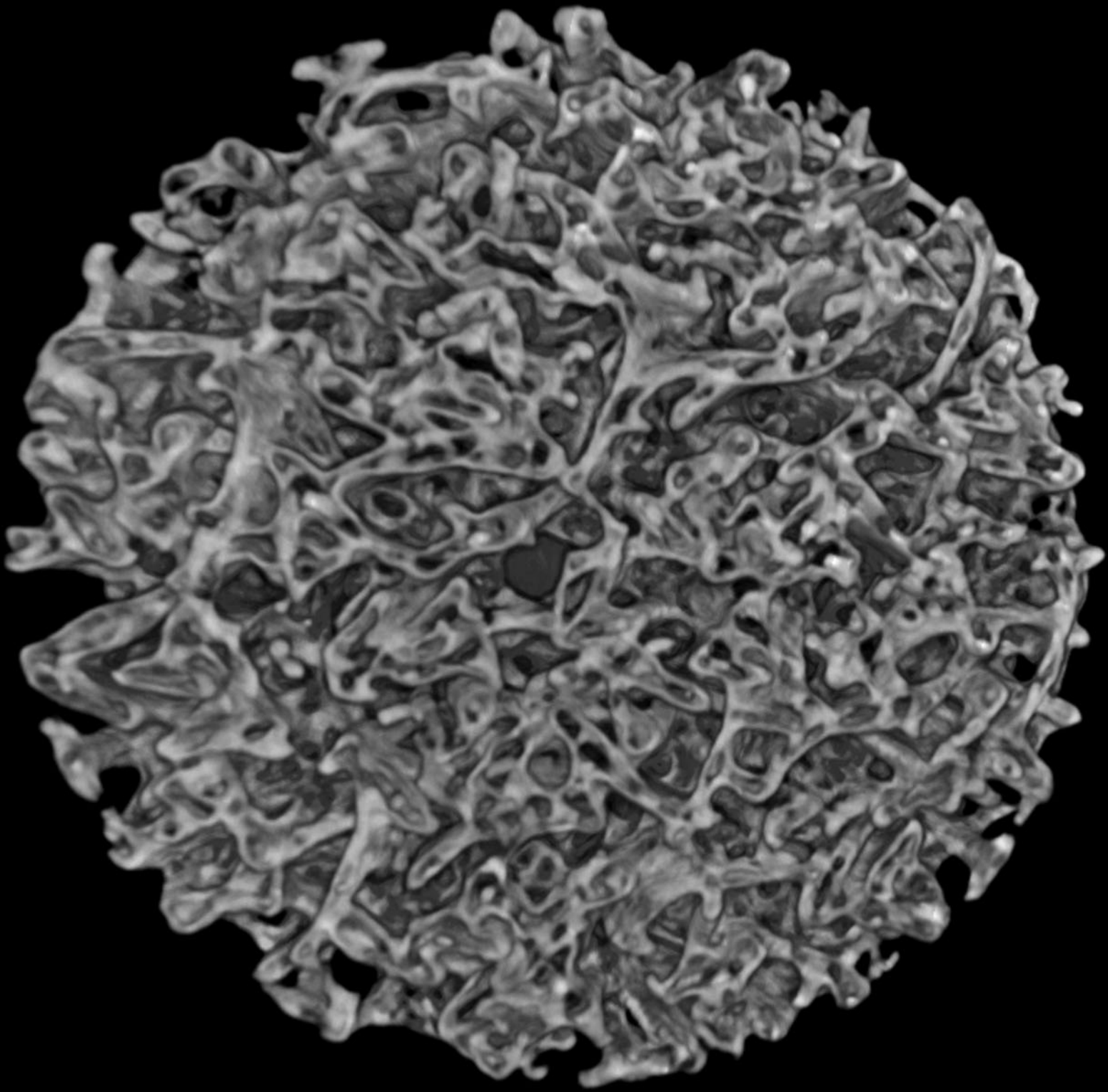

3D PRINTING AND ADDITIVE MANUFACTURING
Volume 3, Number 1, 2016
© Mary Ann Liebert, Inc.
DOI: 10.1089/3dp.2015.0038

*ORIGINAL ARTICLE*

# Enhanced Osteoblast Response to Porosity and Resolution of Additively Manufactured Ti-6Al-4V Constructs with Trabeculae-Inspired Porosity

Alice Cheng,[1–3] Aiza Humayun,[4] Barbara D. Boyan,[1,4,*] and Zvi Schwartz[4,5]

## Abstract

The addition of porosity to the traditionally used solid titanium metal implants has been suggested to more closely mimic the natural mechanical properties of bone and increase osseointegration in dental and orthopedic implants. The objective of this study was to evaluate cellular response to three-dimensional (3D) porous Ti-6Al-4V constructs fabricated by additive manufacturing using laser sintering with low porosity (LP), medium porosity (MP), and high porosity (HP) with low resolution (LR) and high resolution (HR) based on a computed tomography scan of human trabecular bone. After surface processing, construct porosity ranged from 41.0% to 76.1%, but all possessed micro-/nanoscale surface roughness and similar surface chemistry containing mostly Ti, O, and C. Biological responses (osteoblast differentiation, maturation, and local factor production) by MG63 osteoblast-like cells and normal human osteoblasts favored 3D than two-dimensional (2D) solid constructs. First, MG63 cells were used to assess differences in cell response to 2D compared to LR and HR porous 3D constructs. MG63 cells were sensitive to porosity resolution and exhibited increased osteocalcin (OCN), vascular endothelial growth factor (VEGF), osteoprotegerin (OPG), and bone morphogenetic protein 2 (BMP2) on HR 3D constructs than on 2D and LR 3D constructs. MG63 cells also exhibited porosity-dependent responses on HR constructs, with up to a 6.9-fold increase in factor production on LP-HR and MP-HR constructs than on HP-HR constructs. NHOsts were then used to validate biological response on HR constructs. NHOsts exhibited decreased DNA content and alkaline phosphatase activity and up to a 2.9-fold increase in OCN, OPG, VEGF, BMP2, and BMP4 on 3D HR constructs than on 2D controls. These results indicate that osteoblasts prefer a 3D architecture than a 2D surface and that osteoblasts are sensitive to the resolution of trabecular detail and porosity parameters of laser-sintered 3D Ti-6Al-4V constructs.

## Introduction

Additive manufacturing in the biomedical space has traditionally been limited to polymer printing through a deposition style method.[1] In contrast, methods such as laser sintering and electron beam melting manufacture from a bed of powder.[2] These methods allow for a bottom-up manufacturing approach for metals, opening up vast opportunities for engineering implants and devices with improved mechanical strength.

Titanium and its alloys are commonly used materials for orthopedic and dental implants because of their corrosion resistance, high-strength-to-weight ratio, and ability to osseointegrate with the body.[3,4] Until recently, these implants have been manufactured through a reductive process to produce a solid implant body. Although the implant body has not changed much over the past few decades, advances in surface technology have introduced micron scale, submicron scale, and nanoscale roughness as well as increased wettability on implant surfaces. These changes at the surface have helped to increase early osseointegration and implant success in patients.[5,6] However, osseointegration rates still vary widely, especially for patients with diabetes, smokers, and

[1]Department of Biomedical Engineering, Georgia Institute of Technology, Atlanta, Georgia.
[2]Department of Biomedical Engineering, Emory University, Atlanta, Georgia.
[3]Department of Biomedical Engineering, Peking University, Beijing, China.
[4]Department of Biomedical Engineering, Virginia Commonwealth University, Richmond, Virginia.
[5]Department of Periodontics, University of Texas Health Science Center at San Antonio, San Antonio, Texas.

*Opposite page:* High resolution microCT image of implants produced by additive manufacturing. Ti-6Al-4V construct with a 3D trabecular bone inspired porosity.

the elderly.[7–9] In addition, mechanical mismatch in orthopedic implants between the implant bone and host bone can cause stress shielding, leading to repercussions such as increased fracture rates occurring distal to the implant.[10,11] All these factors contribute toward a need for implants that enhance clinical success.

The introduction of porous implants by additive manufacturing has sought to address these issues. This solution is attractive for its ability not only to manufacture materials with less time and waste but also to design custom implants for patients.[12–14] Laser sintering is one form of additive manufacturing that has been used to create bone-interfacing Ti-6Al-4V implants.[13] Already, these laser-sintered solid implants have shown promise in clinical studies.[15] Surface processing methods have been used to achieve similar surface roughness and wettability for additively manufactured Ti-6Al-4V implant materials as traditional implants.[16] Previous studies have shown increased osteoblast-like response to trabecular bone-like constructs based on porosity.[17] Enhanced cell response at the surface can lead to favorable clinical responses. Other porous TI-6Al-4V implants have shown success through increased bone-to-implant contact and mechanical integration than solid implants in animal studies.[18,19] However, as porosity of an irregular bone-like trabecular environment can be difficult to define, cell response may depend on more than just how much void space is available within the construct. The combination of well-known surface parameters such as roughness and hydrophilicity with variations in trabecular detail and porosity has not yet been explored.

In this study, we characterize and evaluate biological response to laser-sintered Ti-6Al-4V constructs with a three-dimensional (3D) trabecular bone-inspired porosity. We hypothesize that osteoblastic response will be enhanced on 3D than on two-dimensional (2D) solid constructs, and that this response is porosity and resolution dependent.

## Materials and Methods

### *Material manufacturing and postfabrication surface processing*

2D disks and 3D constructs were manufactured using laser sintering (EOS GmbH, Krailling, Germany) from Ti-6Al-4V powder as described previously.[17] 2D disks were 15 mm in diameter and 1 mm in height. A computed tomography (CT) template scan was taken of human femoral trabecular bone ($\mu$CT40; Scanco Medical, Bassersdorf, Switzerland) with a 16 $\mu$m voxel size. Scanco software was used to rotate the template on itself 12, 24, or 36 times to create low porosity (LP), medium porosity (MP), or high porosity (HP) constructs 15 mm in diameter and 5 mm in height, which included a 1 mm solid base. In this study, resolution is defined as the amount of trabecular detail captured from the original CT scan. ''High-resolution'' constructs are those that captured more detail from the CT template because of higher thresholding within the capture software. ''Low-resolution'' constructs are those with a lower data capture threshold and resulted in less detail incorporated into the final manufactured construct. Disks and constructs were blasted with $CaPO_4$ particles, followed by acid etching once in 0.3N $HNO_3$ at 45°C and twice at 25°C for 5 min. Materials were rinsed in 97% methanol before ultrasonicating three times for 10 min in ultrapure distilled water at room temperature. Materials were then immersed for 30 min at 80°C in a 1:1 solution of 20 g/L NaOH and 20 g/L $H_2O_2$ and ultrasonicated again in water at room temperature. Materials were finally immersed in 65% $HNO_3$ for 30 min before ultrasonicating in water at room temperature. All materials were allowed to dry for at least 24 h to stabilize the oxide layer, then sterilized by gamma irradiation before characterization and cell culture.

### *Material characterization*

Scanning electron microscopy (SEM) was used to evaluate surface topography at the macro-, micro- and submicro/nanoscales (Zeiss AURIGA, Oberkochen, Germany). Images were taken using a 4 kV accelerating voltage, 30 $\mu$m aperture, InLens detector, and 4 mm working distance.

Microcomputed tomography (microCT) was used to evaluate porosity of 3D constructs (SkyScan 1173; Bruker Corporation, Billerica, MA). An accelerating voltage of 100 kV, current of 80 $\mu$A, 1.0 mm aluminum filter, and pixel size of 20.1 $\mu$m were used to image constructs. Files were reconstructed in NRecon software with 100% beam hardening. Reconstructed files were analyzed in CTAn software to determine total porosity (percentage of void space within construct), surface area-to-volume ratio (SA/V), pore diameter (average spherical diameter between metal struts), and strut thickness. The average ± standard deviation (SD) of porosity parameters was calculated for six samples per group.

Laser confocal microscopy (LCM) was used to image and quantify surface roughness (Zeiss LSM 710). Z-stacks were obtained with a Plan Apochromat 20×/0.8 M27 objective with a 5× optical zoom, 0.39 $\mu$s pixel dwell, 25 $\mu$m pinhole, 85 × 85 $\mu$m image size, and z-step of 1 $\mu$m. A 405 nm laser with 50% strength was used in reflection mode. 3D z-stack images were captured of 2D and 3D constructs at 10× magnification to show differences in macroscale features. To evaluate surface roughness, z-stacks were taken at 40× magnification with a 5× optical zoom to eliminate interference from curvature. Average surface roughness (Sa) was defined as the average absolute distance in the z-plane, and peak-to-valley height (Sz) was defined as the average sum of the highest peak and the lowest valley in the z-plane. Roughness values were obtained using ZEN software (Zeiss) and shown as an average ± SD of six samples per group.

X-ray photoelectron spectroscopy (XPS) was used to analyze surface chemistry (ThermoFisher ESCALab 250). Analysis was conducted using an XR5 gun at 15 kV with a 20 ms dwell time and 1 eV energy step size. A spot size of 500 $\mu$m was used, with average values taken from two survey scans.

Sessile drop contact angle analysis was used to determine surface wettability on 2D disks (Ramé-Hart Instrument Co., Succasunna, NJ). A 4 $\mu$L drop of distilled water was placed on disks, and the left and right angles were averaged every 5 s for 20 s after drop placement. A total of $n = 10$ drops were analyzed across two disks.

Mechanical properties of samples were evaluated through compression testing of porous constructs (MTS Insight 30; MTS Systems Corporation, Eden Prairie, MN) at room temperature. Testing was conducted with a speed of 0.02 mm/s, data acquisition rate of 500 hz/s, preload of 0.01 kN, preload speed of 0.025 mm/s, and strain endpoint of 80%. Testing

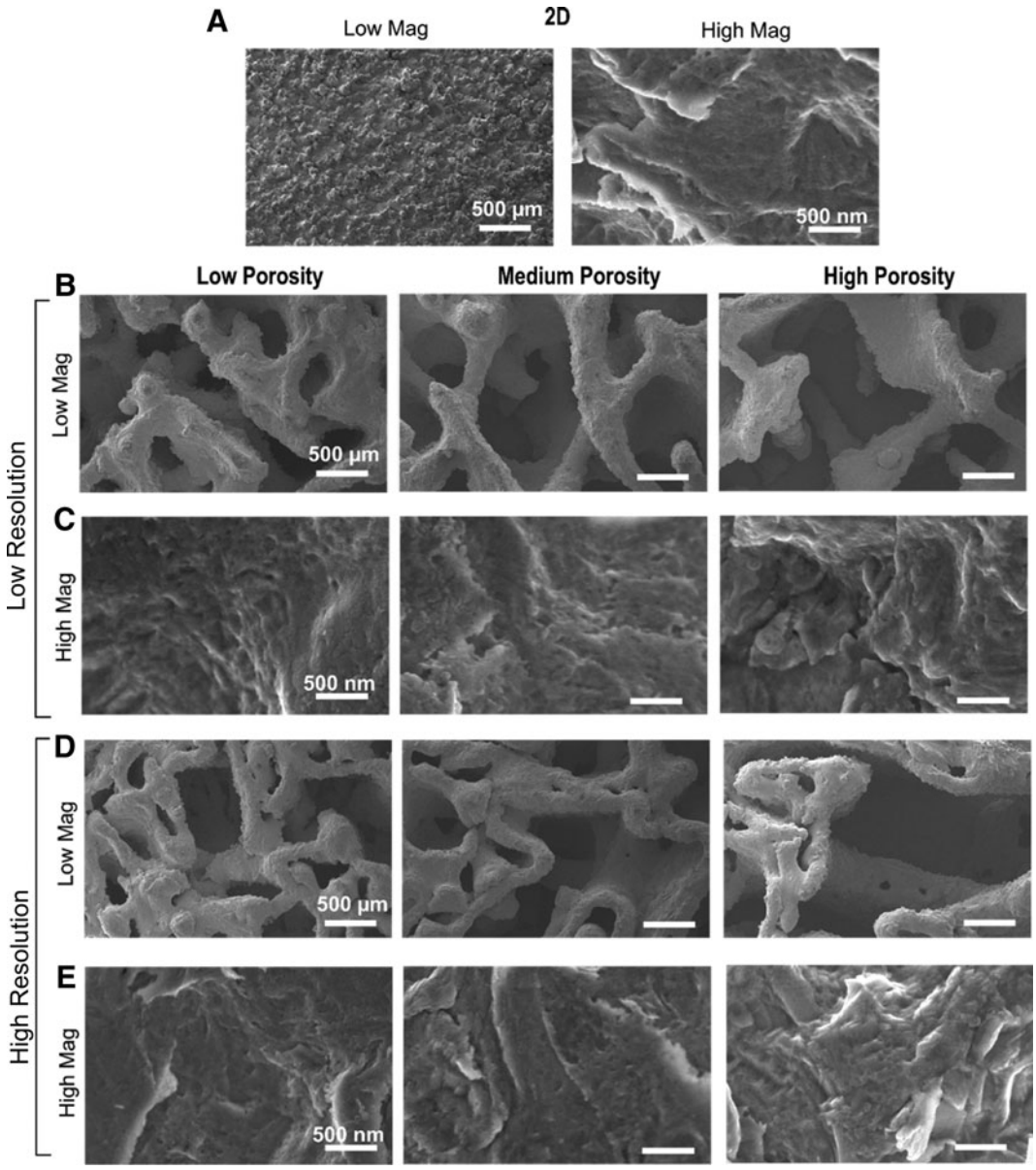


FIG. 1. Scanning electron micrographs of 2D **(A)**, low-resolution 3D **(B, C)** and high-resolution 3D **(D, E)** constructs. Low magnification (**A** [*left*], **B**, **D**) shows macrostructure of constructs, whereas high magnification (**A** [*right*], **C**, **E**) shows micro- and nanoroughness of surfaces. 2D, two-dimensional; 3D, three-dimensional.

was conducted until failure or a 30 kN maximum load was applied.

### *Biological response*

MG63 osteoblast-like cells (ATCC, Manassas, VA) and normal human osteoblasts (NHOst Donor 25433, Lot 336963; Lonza, Walkersville, MD) were cultured to confluence in T75 flasks before plating. 2D disks and 3D constructs were designed to fit snugly in the bottom of a 24-well plate. Cells were plated at a density of 30,000 cells/cm$^2$ according to surface area on tissue culture polystyrene, which was used as an optical control for confluence. Cells were fed with full medium (DMEM +10% FBS +1% penicillin/streptomycin) 24 h after plating. At confluence at approximately day 3, cells were treated with fresh medium and harvested 24 h afterward for analysis of cell layer lysate and conditioned medium.

DNA content was analyzed by fluorescence using the Quant-iT kit (Thermo Fisher Scientific, Waltham, MA). Alkaline phosphatase (ALP) specific activity of cell lysates was determined by analyzing release of para-nitrophenol from para-nitrophenolphosphate at pH 10.2. ALP was normalized to total protein content as determined by bicinchoninic acid assay (Thermo Fisher Scientific). Enzyme-linked immunosorbent assays were used to evaluate expression of osteocalcin (OCN; Alfa Aesar, Ward Hill, MA), osteoprotegerin (OPG, R&D Systems, Inc., Minneapolis, MN), vascular endothelial growth factor (VEGF, R&D Systems, Inc.), and bone morphogenetic proteins 2 and 4 (BMP2; PeproTech, Rocky Hill, NJ, and BMP4; R&D Systems, Inc.).

Table 1. Porosity Parameters Obtained by MicroCT (Average ± Standard Deviation)

| Group | Total porosity (%) | SA/V ratio | Pore diameter (μm) | Strut thickness (μm) |
|---|---|---|---|---|
| Low resolution | | | | |
| 3DLP | 41.0 ± 0.3 | 5.1 ± 0.1 | 641 ± 9 | 673 ± 10 |
| 3DMP | 56.6 ± 2.4[a] | 6.5 ± 0.3[a] | 785 ± 15[a] | 572 ± 18[a] |
| 3DHP | 76.1 ± 0.8[a,b] | 8.1 ± 0.1[a,b] | 1096 ± 31[a,b] | 475 ± 7[a,b] |
| High resolution | | | | |
| 3DLP | 52.5 ± 2.1[a–c] | 10.2 ± 0.2[a–c] | 461 ± 9[a–c] | 311 ± 6[a–c] |
| 3DMP | 57.3 ± 0.8[a,c,d] | 10.8 ± 0.3[a–d] | 563 ± 2[a–d] | 288 ± 8[a–d] |
| 3DHP | 70.9 ± 0.4[a–e] | 11.5 ± 0.1[a–e] | 872 ± 6[a–e] | 267 ± 3[a–e] |

One-way ANOVA with Bonferroni correction, $p < 0.05$.
[a]Versus LP-LR.
[b]Versus MP-LR.
[c]Versus HP-LR.
[d]Versus LP-HR.
[e]Versus MP-HR.
LP, low porosity; MP, medium porosity; HP, high porosity; LR, low resolution; HR, high resolution.

### Statistics

All material characterization results are shown as average and SD, whereas biological results are shown as average and standard error of the mean (SE). The differences between groups of three or more were measured by one-way analysis of variance (ANOVA) that was performed with a Bonferroni *post hoc* analysis. $p < 0.05$ was considered statistically significant.

## Results

### Material characterization

SEM images of sintered constructs showed varying macroscale topography but similar micro-/submicro-/nanoscale topography after surface processing. 2D controls possessed pronounced peaks observed at low magnification, whereas microroughness with nanofeatures was evident at high magnification (Fig. 1A). Macroscale features of 3D constructs with low resolution (LR) (Fig. 1B) were significantly different than those with high resolution (HR) (Fig. 1D). 3D constructs with HR contained smaller pores and struts within larger features. However, high-magnification images of all 2D and 3D constructs across porosities and resolutions indicated similar microroughness, which included submicron and nanofeatures (Fig. 1C, E).

MicroCT analysis showed that total porosity was 41.0%, 56.6%, and 76.1% for LP-LR, MP-LR, and HP-LR constructs, respectively. Total porosity was 52.5%, 57.3%, and 70.9% for LP-HR, MP-HR, and HP-HR constructs, respectively (Table 1). Total porosity values were not significantly different than open porosity values for the same constructs (Fig. 2A). Cross-sectional images of constructs showed finer detail in HR constructs than in LR constructs, which was evident throughout the bulk of the construct (Fig. 2B). MicroCT analysis also showed that SA/V ratio and pore diameter increased and strut thickness decreased with increasing porosity for both LR and HR constructs (Table 1). SA/V ratio ranged from 5.1 to 8.1 for LR constructs and from 10.2 to 11.5 for HR constructs. Pore diameter ranged from 641 to 1096 μm for LR constructs and from 461 to 872 μm for HR constructs. Strut thickness ranged from 475 to 673 for LR constructs and from 267 to 311 for HR constructs.

Surface roughness was evaluated by LCM (Fig. 2C–E). Sa was not significantly different for any of the 2D or 3D construct surfaces. Peak-to-valley height values did not differ for any surfaces except for 3DHP-HR, the values of which were higher than those for 3DMP-LR.

XPS showed that a majority of elements present on the surface of 2D and 3D LR constructs were oxygen (O), carbon (C), and titanium (Ti). The levels of these three main elements did not vary significantly between 2D and 3D constructs (Fig. 3A). Differences were exhibited for lower concentration elements nitrogen (N) and sulfur (S). 2D surfaces possessed a contact angle of 62 ± 18° (Fig. 3B).

Compression testing showed a nonlinear decrease in compressive modulus with increasing construct porosity, with different trends for changes in porosity in LR and HR constructs (Fig. 3C). Average compressive moduli of 3.6 ± 0.083, 3.4 ± 0.080, and 2.6 ± 0.078 GPa decreased significantly as porosity increased for LP-LR, MP-LR, and HP-LR constructs, respectively. A similar trend was observed for LP-HR, MP-HR, and HP-HR constructs with respective compressive moduli of 4.1 ± 0.024, 3.8 ± 0.058, and 2.4 ± 0.15 GPa.

### Cell response

MG63 cells exhibited differential responses to 2D and LR and HR 3D constructs. MG63 cells exhibited porosity- and resolution-dependent responses to 3D constructs. DNA content decreased for all 3D constructs compared with that for 2D surfaces (Fig. 4A). DNA content was further decreased for LP-HR and MP-HR constructs than for all LR constructs, and DNA content increased for HP-HR constructs than for LP-HR and MP-HR constructs. OCN was elevated on HP-LR, LP-HR, and MP-HR constructs than on 2D surfaces and LP-LR constructs (Fig. 4B). OCN for LP-HR and MP-HR constructs was additionally increased than for MP-LR and HP-LR constructs. OPG was elevated on LP-HR and LP-HR constructs than on 2D surfaces, and OPG was elevated on LP-HR than on LP-LR and MP-LR constructs (Fig. 4C). OPG was decreased on MP-HR and HP-HR constructs than on LP-HR constructs. VEGF was increased on HP-LR and MP-HR constructs than on 2D surfaces and LP-LR and MP-LR constructs, and VEGF on MP-HR was also increased than on HP-LR and LP-HR constructs (Fig. 4D). BMP2 was increased on HP-LR, LP-HR, and MP-HR constructs than on 2D surfaces, LP-LR, and MP-LR constructs and decreased on HP-HR constructs than on HP-LR, LP-HR, and MP-HR constructs (Fig. 4E).

NHOst response to 2D versus 3D constructs confirmed the MG63 cell results. Therefore, effects of porosity were only analyzed on HR constructs. NHOsts grown on HR constructs exhibited less robust differences to porosity on HR constructs than MG63 cells. DNA content and ALP activity were decreased on all 3D constructs compared with those on 2D surfaces (Fig. 5A, B). Osteocalcin was significantly higher on LP-HR and MP-HR constructs than on 2D surfaces, whereas OPG, VEGF, and BMP4 were elevated on all 3D constructs compared with those on 2D surfaces (Fig. 5D, E, G). BMP2

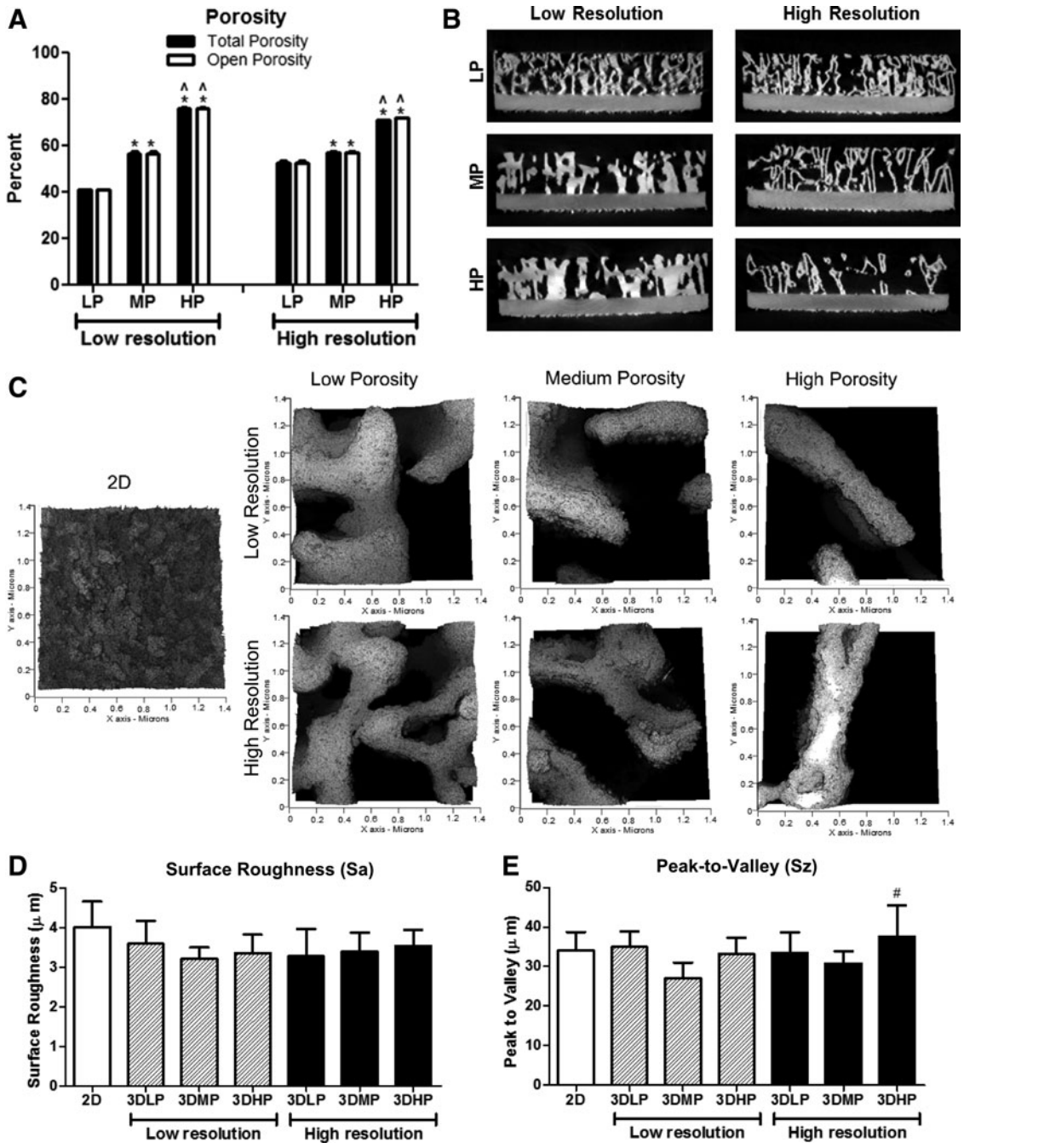


FIG. 2. Total (*black*) and open (*white*) porosity values **(A)** and cross-sectional views **(B)** of 3D constructs obtained by microCT imaging. One-way ANOVA with Bonferroni correction, $p < 0.05$, *versus LP, ^versus MP within low-and high-resolution groups. Student's *t*-test comparing total and open porosity for each group was not significant. Surface roughness images **(C)** and average surface roughness **(D)** and peak-to-valley height values **(E)** for 2D surfaces and 3D constructs. One-way ANOVA with Bonferroni correction, $p < 0.05$, #versus 3DMP-LR. LP, low porosity; MP, medium porosity; LR, low resolution;

was elevated on all 3D constructs compared with that on 2D surfaces but was decreased on HP-LR constructs compared with that on MP-HR constructs (Fig. 5F).

## Discussion

Total and open porosity of 3D constructs did not differ, indicating that all pores were interconnected. MicroCT results corroborated qualitative SEM observations. Although MP-LR and MP-HR constructs did not have significantly different total porosity values, MP-HR constructs had a significantly higher SA/V ratio and smaller pore diameter and smaller strut thickness than 3DMP-LR constructs. This could also be observed in SEM images and was due to the incorporation of higher detail into 3DMP-HR constructs.

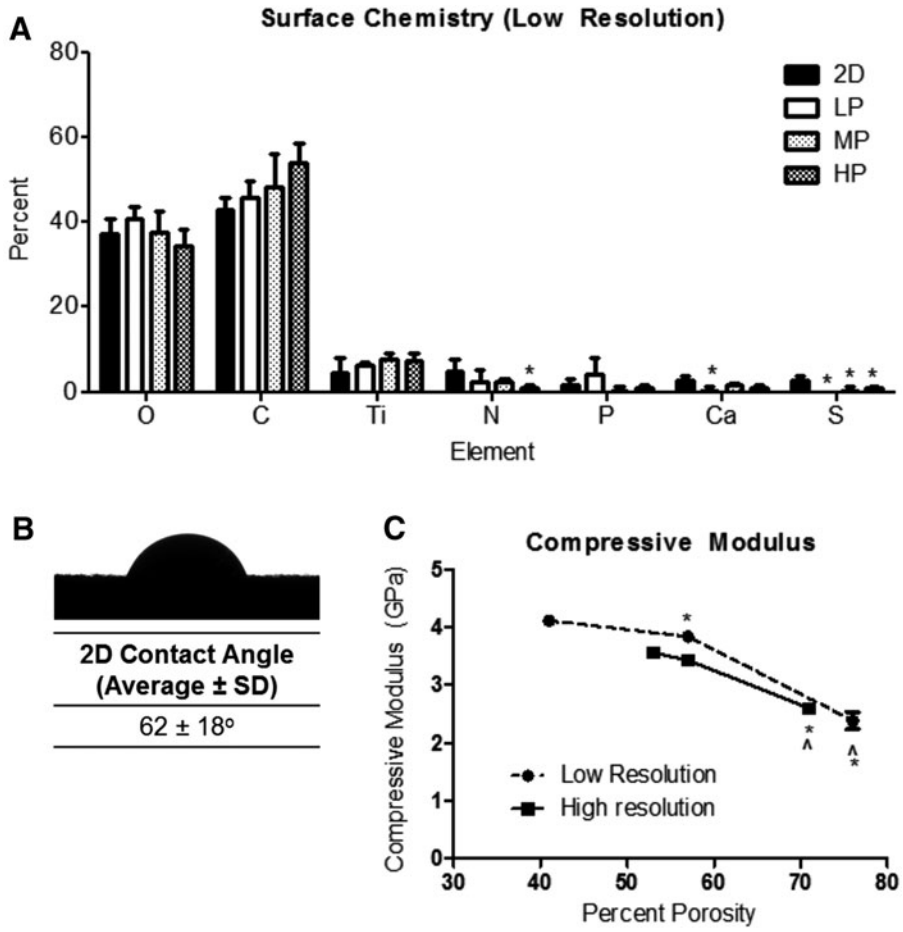


FIG. 3. Surface chemistry of 2D and 3D high-resolution constructs **(A)**. One-way ANOVA with Bonferroni correction, $p < 0.05$, *versus 2D. Contact angle of 2D surfaces **(B)**. Average and standard deviation of compressive modulus values for low-resolution (*circles*, *dotted line*) and high-resolution (*squares*, *solid line*) 3D constructs **(C)**. One-way ANOVA with Bonferroni correction, $p < 0.05$, *versus low porosity, ^versus medium porosity for each type of resolution.

Although Sa did not differ for constructs, peak-to-valley heights did vary for some. This may have been because of the inability of line-of-sight surface processing techniques to evenly affect and penetrate all parts of the constructs. Although acid etching may be able to penetrate the entire construct, blasting by calcium phosphate may have been limited to certain exposed sites at the surface. Cross-sectional SEM images shown in a previous study corroborate this.[17]

Although high-concentration Ti, O, and C elements did not vary across constructs, the presence of low-concentration elements did differ. Variations in nitrogen may be a result of time spent during manufacturing and surface processing, as nitrogen is used in the laser sintering process as well as during etching in $HNO_3$. The presence of Ca and P could be attributed to trace elements left behind during blasting with $CaPO_4$. Although XPS analysis was averaged across six different areas and multiple constructs, differences in one area may contribute to a larger SD for low-concentration elements.

Contact angle analysis could not be performed on 3D constructs because of the large pores. Although contact angle was performed on 2D surfaces as a proxy, the surface roughness may have contributed to higher SD in contact angle values.[20] Additional methods for wettability analysis may need to be evaluated in the future to gain a better understanding of surface energy on 3D constructs.

Optimal bone substitution materials should have similar mechanical properties to natural bone and integrate well with the surrounding tissue. In addition to their ability to osseointegrate, titanium alloys are attractive for implant materials because of their high-fracture toughness and strength.[21] However, the high elastic modulus of titanium compared with that of bone can cause significant clinical problems for orthopedic implants. Elastic moduli for bone has been reported to range from 0.5 to 30 GPa based on trabecular or cortical areas, which differs from an elastic modulus of up to 115 GPa for titanium alloys.[22–24] This difference in bulk material properties can lead to insufficient loading on bone distal to the implant, resulting in stress shielding and bone resorption.[10,23] For hip implants in particular, reduced stem stiffness by incorporating porosity can decrease bone atrophy due to stress shielding.[11]

All 3D constructs presented in this study had compressive moduli ranging from 2.4 to 4.1 GPa, which are within the lower range of moduli for bone.[23] Other studies have indicated similar mechanical properties for laser-sintered porous Ti-6Al-4V.[17,25] Differences in mechanical properties of

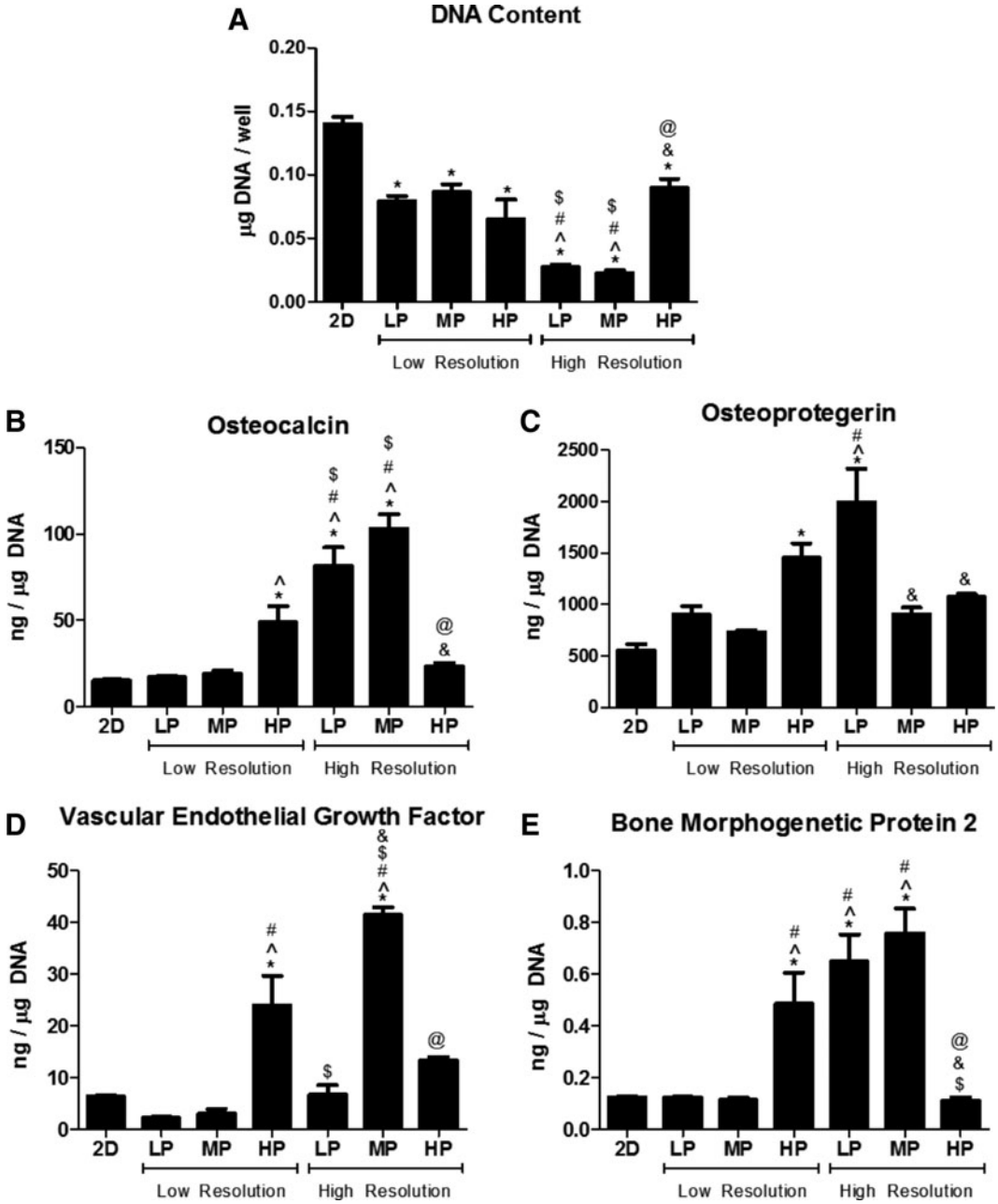


FIG. 4. MG63 cell response to 2D and low- and high-resolution 3D constructs. DNA content **(A)**, osteocalcin **(B)**, osteoprotegerin **(C)**, vascular endothelial growth factor **(D),** and bone morphogenetic protein 2 **(E)**. One-way ANOVA with Bonferroni correction, $p < 0.05$, *versus 2D, ^versus 3DLP-LR, $^{\#}$versus 3DMP-LR, $^{\$}$versus 3DHP-LR, $^{\&}$versus 3DLP-HR, $^{@}$versus 3DMP-HR.

constructs and the nonlinear correlation with total porosity can also be attributed to differences in structural parameters such as strut size and tortuosity.[26,27] These results indicate that porosity can be tailored to alter mechanical properties for patient- and application-specific implants, with the potential to reduce stress shielding. In this study, compression testing was performed to evaluate the elastic modulus. Although tensile modulus is typically reported for materials, previous studies have shown that compressive and tensile analyses of bone yield comparable modulus values.[28] In addition, the load-bearing nature of bone-interfacing implants makes compression testing more clinically relevant. Because compression testing was performed on constructs which included a 1 mm solid base, modulus values may be higher than for completely porous constructs. However, the values presented here may be more clinically relevant for solid implants coated with a porous exterior.

Various studies have shown increased osseointegration through volume of bone ingrowth and mechanical stability of porous implants compared with that of solid implants.[19,29,30] Our hope is that porosity inspired by nature would yield a better biological response than human-designed porosity. We have seen this concept to be true in previous studies of surface roughness, where osteoblasts exhibit higher factor production

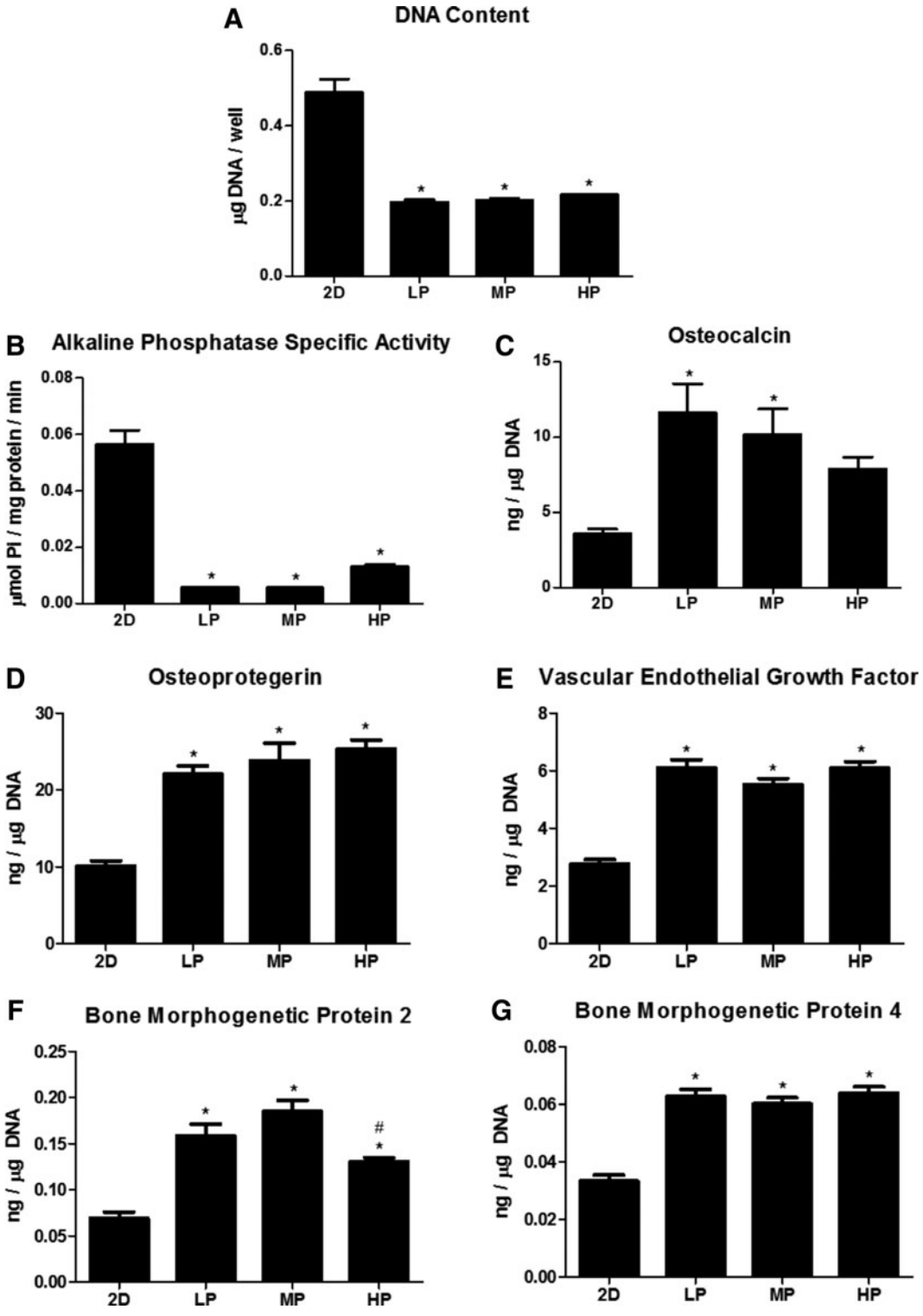


FIG. 5. Normal human osteoblast response to 2D and high-resolution 3D constructs. DNA content **(A)**, alkaline phosphatase specific content **(B)**, osteocalcin **(C)**, osteoprotegerin **(D)**, vascular endothelial growth factor **(E)**, bone morphogenetic protein 2 **(F),** and bone morphogenetic protein 4 **(G)**. One-way ANOVA with Bonferroni correction, $p < 0.05$, *versus 2D, #versus MP.

on acid-etched and grit-blasted titanium surfaces with a more natural distribution of peaks and valleys than micro-patterned substrates with predefined features.[31] Other studies have shown the effectiveness of combined micro-/nanoroughness on titanium substrates, mimicking the natural hierarchical surface roughness of bone, for improving osteoblast response.[32,33] Through characterization data, we showed that our constructs had similar surface chemistry and multiscale roughness but differences in 3D porosity. Based on the differential biological response to our materials, we propose that

osteoblast response is sensitive to and dependent on changes in pore diameter and structure in 3D Ti-6Al-4V constructs.

Osteoblasts showed increased differentiation, maturation, and local factor production on 3D constructs compared to on 2D solid surfaces. In this study, we first used the MG63 cell line to screen for differences in biological response to 2D versus 3D constructs with LR and HR. The MG63 osteoblast-like cell line is commonly used to evaluate cell response to titanium surfaces. Although immortalized cell lines are attractive for their ease of culture and reduced biological variability, they cannot serve as a substitute for using primary cells. MG63 cells in particular, although acceptable for pilot testing of biomaterials, still exhibit increased proliferation, *RUNX2*, and *BGLAP* gene expression and decreased *ALPL* and *COL1A1* gene expression compared with normal human osteoblasts.[34] Owing to the clear preference of MG63 cells for HR constructs, we then chose NHOsts as a primary osteoblast to validate MG63 results to changes in porosity only on HR constructs. Although both MG63 and NHOst cells significantly favored 3D porous constructs over 2D solid surfaces, NHOsts exhibited less of a porosity-dependent response on HR constructs compared with that of MG63 cells.

This cell-dependent response to titanium surfaces has been shown previously with respect to surface roughness.[20,35] We propose that this response is also dependent on the stage of osteoblast maturation. A heightened response to various porosities from immature osteoblast-like MG63 cells contrasts a decreased response from NHOsts at a potentially different stage of maturation. Our results showed 6.9-, 6.5-, and 6.1-fold increases in OCN, VEGF, and BMP2 for MG63 cells on MP-HR constructs compared with those on 2D controls, respectively, whereas NHOsts on the same constructs exhibited 2.9-, 2.0-, and 2.7-fold increases, respectively. We have previously observed that mature osteoblasts exhibit a reduced response to surface roughness as well as to 1,25-dihydroxyvitamin D3 treatment compared to less mature osteoblasts.[36]

Age and sex are also important considerations when evaluating response of primary cells and have been shown to significantly affect response to titanium substrates.[37,38] In this study, the NHOst donor was a 2-year-old Caucasian male. It is possible that the young age of this donor resulted in favorable responses to all 3D constructs regardless of porosity, and that an older or more compromised donor would show a more differential response based on porosity. Further studies on primary osteoblast response based on donor age, sex, and potentially health will be necessary to understand whether and how porous constructs can be tailored to certain populations.

Few studies have shown such a clear preference of osteoblasts for 3D porous Ti-6Al-4V constructs over 2D surfaces. Because all materials in this study were manufactured and processed in the same way to achieve similar roughness and chemistry, we propose that the 3D constructs provide a distinct structural advantage over 2D surfaces that increases osteoblast response. It is unclear which specific material parameter drives differentiation of osteoblasts on 3D constructs, if one at all. Previous studies by our laboratory suggest that the enhanced osteoblast response to surface roughness and 3D substrate morphology is dependent upon the $\alpha 2\beta 1$ integrin, a surface receptor for collagen.[39,40] Indeed, changes in porosity may lead to variations in cell attachment and orientation, affecting extracellular matrix production and mineralization.[41] Characterization by microCT shows that total porosity, SA/V, pore diameter, and strut size all vary based on construct design and resolution. However, because of the trabeculae-inspired design of porosity, each of these parameters may change depending on the exact location of characterization. In addition, it is unclear how interconnected porosity affects cell–cell communication.

Not only can open porosity facilitate paracrine signaling but parameters such as size, shape, and tortuosity have also been shown to influence the shear stress on cells.[42] Although mechanical transduction is not well understood in porous constructs, it is well known that changes in the mechanical stimulus of a cell or its substrate can lead to downstream effects.[43] In fact, it is suggested that fluid forces contribute more to osteoblast response than to strain from the substrate or extracellular matrix.[44] Although our characterization provides information on the average porosity parameters for these constructs, cells may experience a different microscale environment based on their location within the construct. Future studies may examine location-specific biological response to understand how response within individual pores contributes to overall biological response.

## Conclusion

Porous Ti-6Al-4V implants have great potential in the dental and orthopedic fields. With additive manufacturing, implant porosity can be customized for the patient. In this study, laser-sintered constructs were manufactured with various porosities and resolution inspired by human trabecular bone structure. Biological response by human osteoblasts showed increased differentiation, maturation, and local factor production on 3D than on 2D solid constructs. Osteoblasts exhibited cell-type-dependent responses to construct porosity. MG63 cells produced higher local factor production on HR than on LR constructs, which incorporated finer detail from trabecular bone. NHOst cells also exhibited an enhanced response to 3D porous constructs than on 2D solids surfaces, though the response to changes in porosity was less evident than that of MG63 cells. These results suggest that incorporating trabecular-inspired porosity into bone-interfacing implants may enhance cellular response and implant osseointegration.

## Acknowledgments

The authors would like to thank Dr. David J. Cohen for his help with microCT analysis, and Illya Kajan for his help with cell culture. Research reported in this publication was supported by the National Institute of Arthritis and Musculoskeletal and Skin Diseases of the National Institutes of Health under Award Number AR052102. The content is solely the responsibility of the authors' and does not necessarily represent the official views of the National Institutes of Health.

## Author Disclosure Statement

Z.S. is a consultant for AB Dental. B.D.B. is a consultant for TitanSpine LLC.

## References

1. Chia HN, Wu BM. Recent advances in 3d printing of biomaterials. J Biol Eng 2015;9:4.
2. van Noort R. The future of dental devices is digital. Dent Mater 2012;28:3–12.

3. Long M, Rack HJ. Titanium alloys in total joint replacement—A materials science perspective. Biomaterials 1998;19:1621–1639.
4. Van Noort R. Titanium: The implant material of today. J Mater Sci 1987;22:3801–3811.
5. Wennerberg A, Albrektsson T. Effects of titanium surface topography on bone integration: A systematic review. Clin Oral Implants Res 2009;20 Suppl 4:172–184.
6. Lang NP, Salvi GE, Huynh-Ba G, *et al.* Early osseointegration to hydrophilic and hydrophobic implant surfaces in humans. Clin Oral Implants Res 2011;22:349–356.
7. Moy PK, Medina D, Shetty V, *et al.* Dental implant failure rates and associated risk factors. Int J Oral Maxillofac Implants 2005;20:569–577.
8. Meldrum RD, Wurtz LD, Feinberg JR, *et al.* Does smoking affect implant survivorship in total hip arthroplasty? A preliminary retrospective case series. Iowa Orthop J 2005; 25:17–24.
9. Jämsen E, Peltola M, Eskelinen A, *et al.* Comorbid diseases as predictors of survival of primary total hip and knee replacements: A nationwide register-based study of 96 754 operations on patients with primary osteoarthritis. Ann Rheum Dis 2013;72:1975–1982.
10. Oh I, Harris WH. Proximal strain distribution in the loaded femur. An in vitro comparison of the distributions in the intact femur and after insertion of different hip-replacement femoral components. J Bone Joint Surg Am 1978;60: 75–85.
11. Sumner DR, Galante JO. Determinants of stress shielding: Design versus materials versus interface. Clin Orthop Relat Res 1992;274:202–212.
12. Jariwala SH, Lewis GS, Bushman ZJ, *et al.* 3d printing of personalized artificial bone scaffolds. 3D Printing Additive Manufac 2015;2:56–64.
13. Mangano F, Chambrone L, van Noort R, *et al.* Direct metal laser sintering titanium dental implants: A review of the current literature. Int J Biomater 2014;2014:461534.
14. Mangano F, Bazzoli M, Tettamanti L, *et al.* Custom-made, selective laser sintering (sls) blade implants as a non-conventional solution for the prosthetic rehabilitation of extremely atrophied posterior mandible. Lasers Med Sci 2013;28:1241–1247.
15. Mangano C, Piattelli A, d'Avila S, *et al.* Early human bone response to laser metal sintering surface topography: A histologic report. J Oral Implantol 2010;36:91–96.
16. Traini T, Mangano C, Sammons RL, *et al.* Direct laser metal sintering as a new approach to fabrication of an isoelastic functionally graded material for manufacture of porous titanium dental implants. Dent Mater 2008;24: 1525–1533.
17. Cheng A, Humayun A, Cohen DJ, *et al.* Additively manufactured 3d porous ti-6al-4v constructs mimic trabecular bone structure and regulate osteoblast proliferation, differentiation and local factor production in a porosity and surface roughness dependent manner. Biofabrication 2014; 6:045007.
18. de Wild M, Schumacher R, Mayer K, *et al.* Bone regeneration by the osteoconductivity of porous titanium implants manufactured by selective laser melting: A histological and micro computed tomography study in the rabbit. Tissue Eng Part A 2013;19:2645–2654.
19. Palmquist A, Snis A, Emanuelsson L, *et al.* Long-term biocompatibility and osseointegration of electron beam melted, free-form-fabricated solid and porous titanium alloy: Experimental studies in sheep. J Biomater Appl 2013; 27:1003–1016.
20. Gittens RA, Olivares-Navarrete R, Cheng A, *et al.* The roles of titanium surface micro/nanotopography and wettability on the differential response of human osteoblast lineage cells. Acta Biomater 2013;9:6268–6277.
21. Rack HJ, Qazi JI. Titanium alloys for biomedical applications. Mater Sci Eng C Mater Biol Appl 2006;26:1269–1277.
22. Geetha M, Singh AK, Asokamani R, *et al.* Ti based biomaterials, the ultimate choice for orthopaedic implants—A review. Prog Mater Sci 2009;54:397–425.
23. Krishna BV, Bose S, Bandyopadhyay A. Low stiffness porous ti structures for load-bearing implants. Acta Biomater 2007;3:997–1006.
24. Parthasarathy J, Starly B, Raman S. A design for the additive manufacture of functionally graded porous structures with tailored mechanical properties for biomedical applications. J Manuf Process 2011;13:160–170.
25. Sallica-Leva E, Jardini AL, Fogagnolo JB. Microstructure and mechanical behavior of porous ti–6al–4v parts obtained by selective laser melting. J Mech Behav Biomed Mater 2013;26:98–108.
26. Roque WL, Alberich-Bayarri A. Tortuosity influence on the trabecular bone elasticity and mechanical competence. In: Tavares JMRS, Natal Jorge R, editors. Developments in medical image processing and computational vision. Switzerland: Springer International Publishing, 2015, pp. 173–191.
27. Parthasarathy J, Starly B, Raman S, *et al.* Mechanical evaluation of porous titanium (ti6al4v) structures with electron beam melting (ebm). J Mech Behav Biomed Mater 2010;3:249–259.
28. Reilly DT, Burstein AH, Frankel VH. The elastic modulus for bone. J Biomech 1974;7:271–275.
29. Ponader S, von Wilmowsky C, Widenmayer M, *et al.* In vivo performance of selective electron beam-melted ti-6al-4v structures. J Biomed Mater Res A 2010;92A:56–62.
30. Maniatopoulos C, Pilliar RM, Smith DC. Threaded versus porous-surfaced designs for implant stabilization in bone-endodontic implant model. J Biomed Mater Res 1986;20: 1309–1333.
31. Zinger O, Zhao G, Schwartz Z, *et al.* Differential regulation of osteoblasts by substrate microstructural features. Biomaterials 2005;26:1837–1847.
32. Gittens RA, McLachlan T, Olivares-Navarrete R, *et al.* The effects of combined micron-/submicron-scale surface roughness and nanoscale features on cell proliferation and differentiation. Biomaterials 2011;32:3395–3403.
33. Gittens RA, Olivares-Navarrete R, Schwartz Z, *et al.* Implant osseointegration and the role of microroughness and nanostructures: Lessons for spine implants. Acta Biomater 2014;10:3363–3371.
34. Czekanska EM, Stoddart MJ, Ralphs JR, *et al.* A phenotypic comparison of osteoblast cell lines versus human primary osteoblasts for biomaterials testing. J Biomed Mater Res A 2014;102:2636–2643.
35. Gittens RA, Olivares-Navarrete R, McLachlan T, *et al.* Differential responses of osteoblast lineage cells to nanotopographically-modified, microroughened titanium–aluminum–vanadium alloy surfaces. Biomaterials 2012;33: 8986–8994.
36. Lohmann CH, Bonewald LF, Sisk MA, *et al.* Maturation state determines the response of osteogenic cells to surface roughness and 1,25-dihydroxyvitamin d3. J Bone Miner Res 2000;15:1169–1180.

37. Olivares-Navarrete R, Raines AL, Hyzy SL, *et al.* Osteoblast maturation and new bone formation in response to titanium implant surface features are reduced with age. J Biomed Mater Res 2012;27:1773–1783.
38. Olivares-Navarrete R, Hyzy SL, Chaudhri RA, *et al.* Sex dependent regulation of osteoblast response to implant surface properties by systemic hormones. Biol Sex Differ 2010;1:4.
39. Olivares-Navarrete R, Raz P, Zhao, G, *et al.* Integrin $\alpha 2\beta 1$ plays a critical role in osteoblast response to micron-scale surface structure and surface energy of titanium substrates. Proc Natl Acad Sci U S A 2008;105:15767–15772.
40. Wang X, Schwartz Z, Gittens RA, *et al.* Role of integrin $\alpha 2\beta 1$ in mediating osteoblastic differentiation on three-dimensional titanium scaffolds with submicron-scale texture. J Biomed Mater Res A 2015;103:1907–1918.
41. Frosch KH, Barvencik F, Lohmann CH, *et al.* Migration, matrix production and lamellar bone formation of human osteoblast-like cells in porous titanium implants. Cells Tissues Organs 2002;170:214–227.
42. Botchwey EA, Pollack SR, El-Amin S, *et al.* Human osteoblast-like cells in three-dimensional culture with fluid flow. Biorheology 2003;40:299–306.
43. Kapur S, Baylink DJ, William Lau KH. Fluid flow shear stress stimulates human osteoblast proliferation and differentiation through multiple interacting and competing signal transduction pathways. Bone 2003;32:241–251.
44. Owan I, Burr DB, Turner CH, *et al.* Mechanotransduction in bone: Osteoblasts are more responsive to fluid forces than mechanical strain. Am J Physiol 1997;273:C810–C815.

Address correspondence to:
*Barbara D. Boyan*
*Department of Biomedical Engineering*
*Virginia Commonwealth University*
*601 West Main Street*
*Richmond, VA 23284*

*E-mail:* bboyan@vcu.edu